

# Geophysical Research Letters®



## RESEARCH LETTER

10.1029/2025GL115055

## Signal and Noise in the Atlantic Meridional Overturning Circulation at 26°N

Gerard D. McCarthy<sup>1</sup> , Guillaume Hug<sup>1</sup> , David Smeed<sup>2</sup> , Kirsty J. Morris<sup>1</sup>, and Ben Moat<sup>2</sup> 

<sup>1</sup>ICARUS (Irish Climate Analysis and Research Units), Department of Geography, Maynooth University, Maynooth, Ireland, <sup>2</sup>National Oceanography Centre, Southampton, UK

### Key Points:

- There is a weakening of 1.0 Sv/decade from 2004 to 2023 in the Atlantic meridional overturning circulation (AMOC) as observed by the RAPID array
- Low frequency variability is concentrated in the thermocline and Lower North Atlantic Deep Water, reflected in deep hydrography
- Noise levels can be lowered by 20%–30% by regressing out the influence of Ekman transport

### Supporting Information:

Supporting Information may be found in the online version of this article.

### Correspondence to:

G. D. McCarthy,  
[gerard.mccarthy@mu.ie](mailto:gerard.mccarthy@mu.ie)

### Citation:

McCarthy, G. D., Hug, G., Smeed, D., Morris, K. J., & Moat, B. (2025). Signal and noise in the Atlantic meridional overturning circulation at 26°N. *Geophysical Research Letters*, 52, e2025GL115055. <https://doi.org/10.1029/2025GL115055>

Received 28 JAN 2025

Accepted 26 FEB 2025

### Author Contributions:

Writing – review & editing: Kirsty J. Morris

**Abstract** The Atlantic meridional overturning circulation (AMOC) plays a crucial role in redistributing heat within the climate system. The RAPID mooring array has observed an AMOC weakening of 1.0 [0.4–1.6] Sv per decade from 2004 to 2023, consistent with climate model projections and not consistent with a collapse in the mid-21st century. Here, we analyze the AMOC change within a signal-to-noise framework. We find a strong signal in Lower North Atlantic Deep Water (LNADW) and thermocline transports. By removing the influence of Ekman transport on AMOC and LNADW estimates, we reduce noise by 30% and 22%, respectively. Moreover, we demonstrate that a simple model of LNADW yields a comparable signal-to-noise ratio to the full AMOC estimate. Ultimately, we conclude that current AMOC trends are unlikely to reach “unfamiliar” (signal-to-noise ratio > 2) or “unknown” (signal-to-noise ratio > 3) thresholds until the 2040s and 2060s, respectively.

**Plain Language Summary** The ocean's Overturning Circulation moves heat northwards in the Atlantic. It is key for the mild climate of western Europe, the position of the tropical rain belt, and other climate patterns. Climate models predict that the Atlantic Overturning Circulation will weaken in the coming century and some statistical models indicate it may collapse. Oceanographers have put systems of instruments into the ocean to monitor this and observe how strong the Atlantic Overturning Circulation is. However, these measurements can be noisy due to, for example, the short term effect of the wind. In this study, we remove some of this noise to improve our ability to detect the underlying climatic change in the Atlantic Overturning Circulation. We find that observing temperature and salinity in the deep ocean is an effective way to detect changes in the Atlantic Overturning Circulation. By reducing the noise in the measurements we will have a better understanding of how the Atlantic Overturning Circulation is changing and thus detect climate-driven change in a timely manner.

## 1. Introduction

The Atlantic meridional overturning circulation (AMOC) is a system of ocean currents that redistributes heat northwards in the Atlantic. A strong AMOC decline would have important consequences for surface temperatures, precipitation, and wind patterns (Bellomo et al., 2021; Jackson et al., 2015). Since the early 2000s, dedicated observing systems have been implemented to monitor the AMOC. A key motivation for these sustained observations of the AMOC is the projection from successive generations of climate models indicating that the AMOC will weaken in response to future anthropogenic climate change. The most recent CMIP6 models estimate a projected AMOC weakening of 0.7–0.9 Sv/decade to 2100 ( $1 \text{ Sv} = 10^6 \text{ m}^3 \text{ s}^{-1}$ ), for low emissions and high emissions scenarios, respectively (Weijer et al., 2020). More abrupt, statistical estimates of collapse by mid-21st century would correspond to an approximate 5 Sv/decade AMOC decline (Ditlevsen & Ditlevsen, 2023) relative to current AMOC strength.

Direct, continuous observations of the AMOC are relatively short in the context of climatic timescales, with dedicated programs for continuous AMOC observation only beginning with the start of the RAPID-MOCHA-WBTS program, during the first decade of the 21st century (Frajka-Williams et al., 2019). Initial results from the RAPID-MOCHA-WBTS (MOCHA: Meridional Overturning Circulation and Heatflux Array; WBTS: Western Boundary Time Series; referred to hereafter as RAPID) project revealed the highly variable nature of the AMOC at 26°N on timescales from days to years (Cunningham et al., 2007; Kanzow et al., 2010; McCarthy et al., 2012; Smeed et al., 2014). RAPID has seen a range of  $-4.3$  to  $32.3$  Sv in the AMOC (10-day filtered values) from April 2004 to January 2023. Understanding of the origins of the variability observed in the AMOC has

© 2025 The Author(s).

This is an open access article under the terms of the [Creative Commons Attribution-NonCommercial](https://creativecommons.org/licenses/by-nc/4.0/) License, which permits use, distribution and reproduction in any medium, provided the original work is properly cited and is not used for commercial purposes.

advanced in the 20 years of RAPID observations, with seasonality (Chidichimo et al., 2010; Kanzow et al., 2010; Pérez-Hernández et al., 2015), interannual variability (McCarthy et al., 2012; Roberts et al., 2013), and the impact of the mesoscale (Evans et al., 2022; Kanzow et al., 2009) all contributing. Surprising relationships have been unearthed, such as the link between Ekman transport (the movement of surface water influenced by the Coriolis effect and wind) at the surface and deepwater transport at 3,000–5,000 m in lower North Atlantic deep water (LNADW) (Frajka-Williams et al., 2016).

High variability has not barred studies from looking at longer term trends in the AMOC. Smeed et al. (2014) found a strong weakening in the first 8 years of RAPID. The weakening AMOC in the RAPID timeseries appeared to end, with a strengthening observed from 2009/2010 to 2018 (Moat et al., 2020). However, the latest data, released in September 2024, shows the AMOC has returned to weakening. Such reversals in AMOC trends during the past 20 years have posed problems for the Intergovernmental Panel for Climate Change (IPCC), with a diluting in the confidence statement associated with observed AMOC decline between the Special Report on Ocean and Cryosphere report and the 6th assessment report ((IPCC, 2019, 2021); see McCarthy and Caesar (2023)) for discussion of this). This makes AMOC a climate variable that, while consistently projected to weaken in response to climate change, has not been observed directly to do so.

The detection of climatic change in observations of the AMOC has also been considered in model-observation frameworks. The study of Baehr et al. (2007) showed deep, basinwide density gradients as a sensitive estimator of AMOC decline due to lower noise in the deep ocean. Roberts et al. (2014) combined the higher variability in observations with trends from climate models to estimate that a decade of observations would be needed to detect climate scale trends. Lobelle et al. (2020) found that, when the high variability in the observations is considered, approximately 4 decades of data would be needed to detect a typical climate trend.

In the context of detection, low-frequency (5-year) variability can be considered the target signal with other observed variability being classed as noise. In this study, we integrate our understanding of the sources of variability in RAPID AMOC estimates with a detectability estimator based on the signal-to-noise ratio. We explore whether there are effective transport components other than the full AMOC estimate for monitoring climatic AMOC change.

## 2. Data and Methods

This study uses monthly, deseasonalized data from the RAPID array (Moat et al., 2024). Utilizing this data we estimate the decorrelation (e-folding of the autocorrelation function) of 1 month (Figure S1 in Supporting Information S1). This is similar to the 40 days value from Smeed et al. (2014), meaning these monthly values can be considered independent. The mean strength of the AMOC is 17.0 Sv with a standard deviation of 2.8 Sv from April 2004 to January 2023. This is an estimate of the maximum of the overturning streamfunction—the most common metric of AMOC strength. A linear fit to the deseasonalized monthly AMOC estimates an overall reduction of  $-1.0$  [ $-0.4$  to  $-1.6$ ] Sv/decade (90% confidence interval, estimated with bootstrapping using 1,000 resamples), which is significant at the 95% level and is consistent with the trend estimate of Volkov et al. (2024). While we can categorize the statistical significance of trends, placing the climatic significance of this trend is more difficult.

One approach to framing the question of whether the strength of the AMOC has changed is to examine the signal-to-noise ratio, where the signal is defined as the low-frequency variation in the AMOC. Signal-to-noise ratio has been a useful indicator of the emergence of climate change signals in local data (Hawkins et al., 2020; Murphy et al., 2023). Here, we apply a similar methodology to investigate the emergence of low frequency climatic oscillations and trends in the RAPID data.

We define the signal-to-noise ratio based on a linear regression model:

$$y(t) = \beta x(t) + \epsilon \quad (1)$$

with  $y(t)$  being the observed variable, such as an individual component transport and  $x(t)$  is the low frequency AMOC. In this study, we use a Loess polynomial fit over 5 years to define the low frequency AMOC. The 5 years filter length was selected following on from experiments with filter lengths ranging from 1 to 20 years. The results showed a strong dependency on filter length for durations of 3 years and shorter. However filter lengths between 5

and 20 years produced similar noise estimates with variations within 0.1 Sv. Based on these finding a 5-year filter was selected (Figure S2 in Supporting Information S1).  $\beta$  is an unknown regression coefficient, and

$$\epsilon \sim \mathcal{N}(0, \sigma^2) \quad (2)$$

is the residual of the linear regression whereby  $\sigma^2$  is the variance and  $\sigma$  is the standard deviation.

There are a number of ways to define the signal of interest. For emergent signals, the value of the variable of interest at a specific point may be chosen. For example, when using a signal to noise framework for the emergence of global temperature in local climate trends, (Hawkins et al., 2020; Murphy et al., 2023) used the end value of their variable of interest:  $\beta x(t = t[end])$ , in their case global mean temperature in 2018. We choose a more conservative definition of

$$\beta m \Delta t, \quad (3)$$

where  $\Delta t$  is the length of the timeseries (20 years) and  $m$  is the trend in the AMOC (1 Sv/decade) and  $\beta$  is the scale factor between the low frequency AMOC and the observed variable. In this case we would define the signal-to-noise ratio (SNR) as

$$\text{SNR} = \frac{\text{signal}}{\text{noise}} = \frac{\beta m \Delta t}{\sigma}. \quad (4)$$

This framework lends itself to consideration of the emergence of specific trends from the noise. We can use this to define an emergence time of

$$\Delta t = \frac{\text{SNR} \sigma}{\beta m}. \quad (5)$$

This timescale can be estimated to equate to a signal-to-noise ratio of 2 for “unfamiliar” and to 3 for “unknown” following Frame et al. (2017).

Ocean transports at the RAPID array are provided in layers that correspond to the transport of different water masses, we consider the observation of the climatic AMOC signal in these components (Figure S3 in Supporting Information S1). Thermocline transport (Therm, 0–800 m depth), Upper North Atlantic Deep Water (UNADW, 1,100–3,000 m), LNADW (3,000–5,000 m) flow southwards. Gulf Stream (GS, estimated by the Florida Current) and Ekman (Ek) flow north. Two Antarctic origin water masses (Intermediate and Bottom Waters) contribute little to the monthly or longer timescale variability. The AMOC is well-represented by the sum of shallow (depth < 1,000 m) components balanced by the deep return of North Atlantic Deep Water.

We also examine specific components with Ekman transport removed. Ekman transport, calculated from wind data, is included in the RAPID AMOC estimate both directly and through a mass compensation term that ensures zero net transport across the section (McCarthy et al., 2015). This results in its signal being reflected in the transport of components such as the thermocline, UNADW, LNADW, and Bottom Water. However, it was also found that Ekman transport influences deep density fields, particularly affecting deep temperature and salinity (Frajka-Williams et al., 2016). In these regions, the hydrographic properties of the deep western boundary, between 3,000 and 5,000 m, show a strong correlation with Ekman transport.

In terms of RAPID components transports, UNADW, LNADW, and the AMOC estimate itself are all significantly ( $p < 0.001$ ) correlated with Ekman transport, with correlations of  $-0.33$ ,  $-0.60$ , and  $0.68$ , respectively. Given the lack of impact of Ekman transport change on climatic timescales (Asbjørnsen & Årthun, 2023; Beadling et al., 2018; Bryden et al., 2024), to reduce the noise in the transports, we remove the influence of Ekman transport from each component by regressing out Ekman transport from that component. We refer to these as Component—Ek for example, AMOC – Ek.

We also consider a simplified model of the LNADW transports to investigate the low-frequency AMOC signal in the deep hydrographic properties. Worthington et al. (2021) showed that LNADW can be described by a combination of deep density (pressure = 3,000 m) on the western boundary of RAPID and Ekman transport. Figure 1a

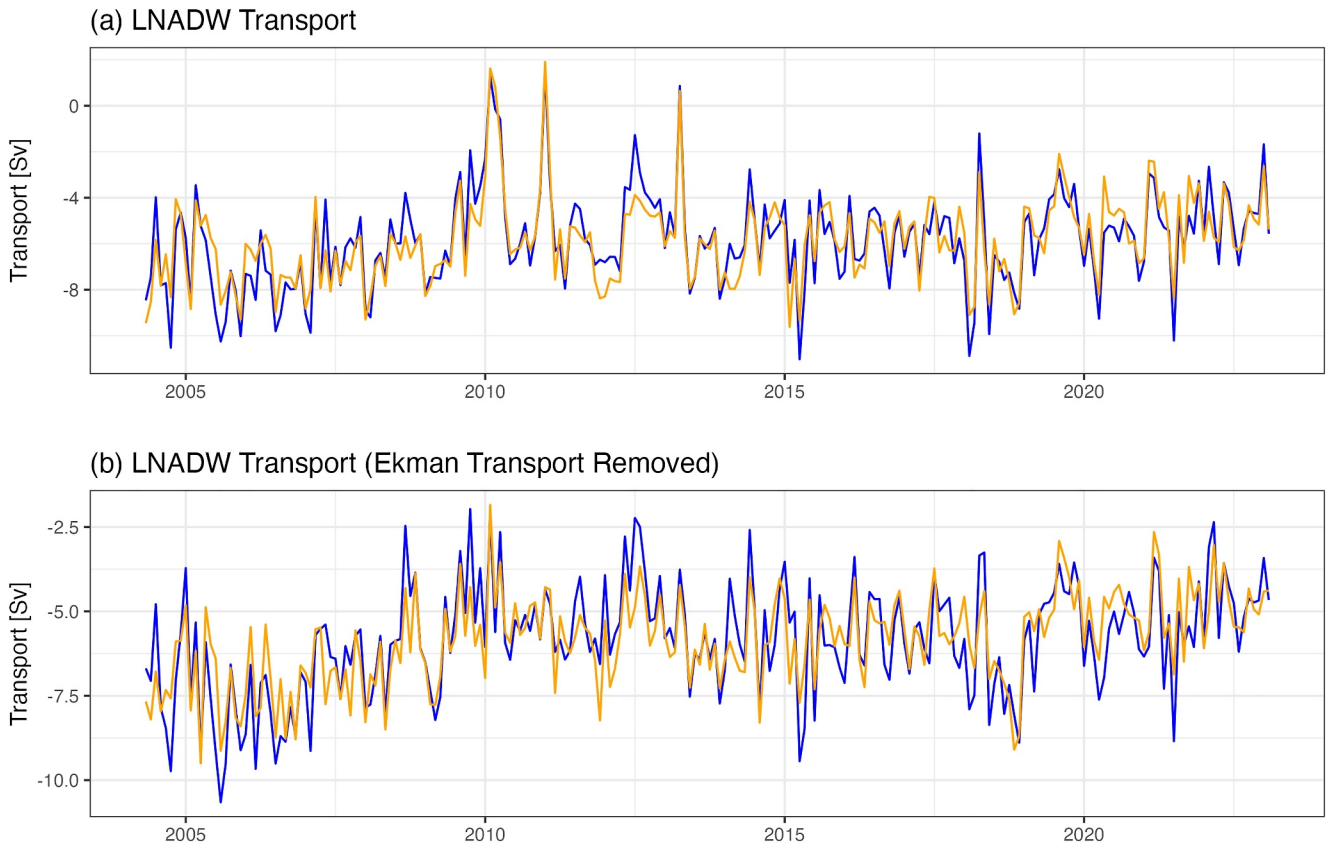


**Figure 1.** (a) Lower North Atlantic Deep Water (LNADW) transport (blue) and LNADW transport estimated from a linear combination of Ekman transport, temperature and salinity at 3,000 m on the western boundary of the RAPID array. (b) LNADW transport with Ekman transport removed by linear regression (blue) and LNADW transport estimated from a linear combination of temperature and salinity at 3,000 m on the western boundary of the RAPID array when Ekman transport had been removed from temperature and salinity via linear regression.

effectively (coefficient of determination:  $r^2 = 0.78$ ) reproduces the generalized least squares model of Worthington et al. (2021) for the LNADW, using western boundary temperature ( $T_{wb}$ ) and salinity ( $S_{wb}$ ) in place of density at a pressure of 3,000 dbar:

$$\text{LNADW}(t) = -0.4 \text{ Ekman}(t) + 32.5 T_{wb}(t) - 2.13 S_{wb}(t), \quad (6)$$

where the coefficients of Ekman transport ( $-0.4$ ) and salinity ( $-2.13$ ) are dimensionless and the coefficient of temperature ( $32.5$ ) has units of  $\text{Sv}/^\circ\text{C}$ .

We also consider a version of this model where initially Ekman transport is removed from  $T_{wb}$ ,  $S_{wb}$ , and LNADW before evaluation of the linear model. This model results in the same coefficients for temperature and salinity indicating the independence of the Ekman relationship and effectively ( $r^2 = 0.6$ ) reproduces the variability of the LNADW – Ek (Figure 1b).

### 3. Results

Figure 2 shows estimation of signal and noise for the AMOC and its components in the RAPID data. The low frequency AMOC signal Figure 2a, shows the decline, recovery, decline pattern previously highlighted with an overall decline of  $1.0$  [ $0.4$ – $1.5$ ]  $\text{Sv}/\text{decade}$  (90% confidence interval). From 2004 to 2023, this signal only begins to emerge from the 1 s.d. envelope shown. This can be considered the “familiar” envelope, with “unfamiliar” emerging at 2 s.d. The AMOC, thermocline, and LNADW components have low frequency signatures that emerge from the 1 s.d. envelope (Figures 2a, 2d, and 2f). The LNADW trend is reversed as it is inverse to the AMOC that is, when the AMOC weakens it corresponds to less northward flow whereas when the LNADW

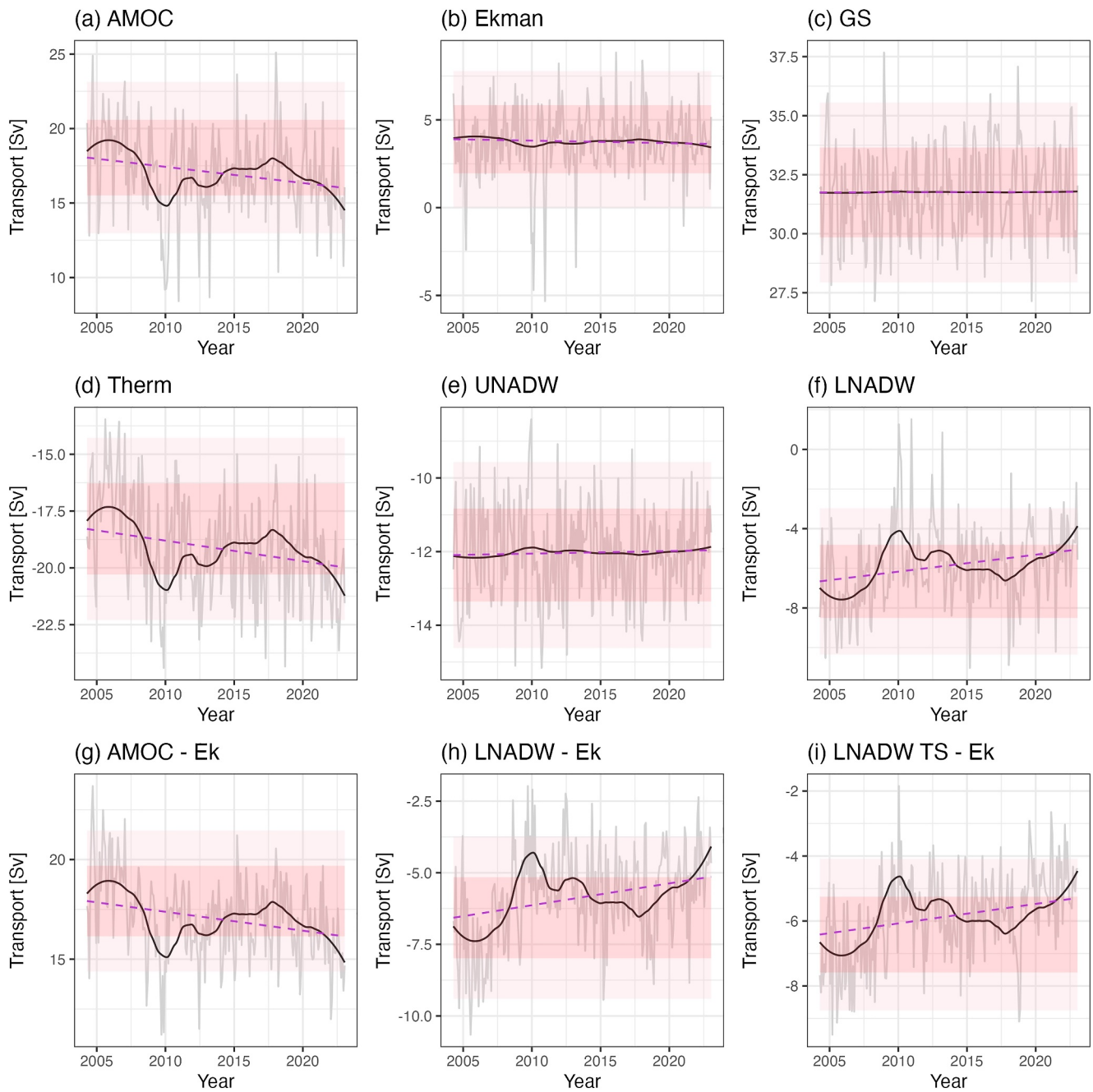


**Figure 2.** Signal to noise in components of the transport at the RAPID array at 26°N. (a) Monthly, deseasonalized Atlantic meridional overturning circulation (AMOC) estimates (gray), low-frequency AMOC signal (black) found by fitting a 5-year Loess filter. The trend of this signal is shown in purple, dashed. For each component (b–f) Ekman, Gulf Stream, thermocline, Upper and Lower North Atlantic Deep Water, the monthly, deseasonalized values (gray) were regressed against the low-frequency AMOC in panel (a). This is shown with the black solid line. Panels (g–i) show the same but with the Ekman transport removed for AMOC, Lower North Atlantic Deep Water, and the latter estimated from temperature and salinity on the western boundary at 3,000 m. The light and dark pink envelopes indicate “noise” estimates for each component at the 2 and 1 s.d. levels.

weakens it results in less southwards flow. The Ekman, GS, and UNADW components do not emerge from the 1 s.d. envelope and do not show a signal significantly different from zero, reflecting these components are not carrying the signature of the low frequency AMOC (Figures 2b, 2c, and 2e). Figures 2g–2i show the effect of removal of Ekman transport from the AMOC, LNADW, and temperature and salinity derived LNADW. Each of these variables continues to reflect the low frequency AMOC signal but with lowered levels of noise.

**Table 1**

*Signal, Noise, Scale Factor, and Derived Components for Atlantic Meridional Overturning Circulation (AMOC), Its Component Transports, and Certain Transports With Ekman Removed Relative to the Low-Frequency AMOC Signal*

	Signal (Sv)	[5%–95% CI]	Noise (Sv)	[5%–95% CI]	S to N Ratio	[5%–95% CI]	Scale factor	[5%–95% CI]	Unfamiliar (Year)	[5%–95% CI]	Unknown (Year)	[5%–95% CI]
<b>LNADW minus Ekman</b>	<b>1.43</b>	<b>[1.75, 1.12]</b>	<b>1.42</b>	<b>[1.3, 1.54]</b>	<b>1.01</b>	<b>[1.06, 0.97]</b>	<b>−0.75</b>	<b>[−0.91, −0.59]</b>	<b>2042</b>	<b>[2039, 2045]</b>	<b>2061</b>	<b>[2056, 2066]</b>
<b>AMOC minus Ekman</b>	<b>1.78</b>	<b>[1.4, 2.2]</b>	<b>1.77</b>	<b>[1.62, 1.95]</b>	<b>1.00</b>	<b>[0.98, 1.02]</b>	<b>0.93</b>	<b>[0.73, 1.15]</b>	<b>2042</b>	<b>[2039, 2046]</b>	<b>2061</b>	<b>[2057, 2067]</b>
<b>LNADW TS minus Ekman</b>	<b>1.13</b>	<b>[1.42, 0.89]</b>	<b>1.17</b>	<b>[1.08, 1.28]</b>	<b>0.96</b>	<b>[1.02, 0.93]</b>	<b>−0.59</b>	<b>[−0.74, −0.46]</b>	<b>2044</b>	<b>[2041, 2047]</b>	<b>2064</b>	<b>[2059, 2069]</b>
<b>LNADW</b>	<b>1.61</b>	<b>[2.07, 1.2]</b>	<b>1.84</b>	<b>[1.68, 2.08]</b>	<b>0.87</b>	<b>[0.92, 0.82]</b>	<b>−0.84</b>	<b>[−1.08, −0.63]</b>	<b>2048</b>	<b>[2044, 2054]</b>	<b>2070</b>	<b>[2064, 2078]</b>
<b>Therm</b>	<b>1.69</b>	<b>[1.25, 2.12]</b>	<b>2.01</b>	<b>[1.84, 2.2]</b>	<b>0.84</b>	<b>[0.83, 0.87]</b>	<b>0.89</b>	<b>[0.66, 1.11]</b>	<b>2049</b>	<b>[2045, 2054]</b>	<b>2072</b>	<b>[2066, 2079]</b>
<b>AMOC</b>	<b>2.04</b>	<b>[1.44, 2.63]</b>	<b>2.54</b>	<b>[2.27, 2.85]</b>	<b>0.80</b>	<b>[0.78, 0.82]</b>	<b>1.07</b>	<b>[0.75, 1.37]</b>	<b>2052</b>	<b>[2047, 2058]</b>	<b>2076</b>	<b>[2068, 2084]</b>
Ekman	0.27	[−0.27, 0.73]	1.94	[1.69, 2.32]	0.14	[0.08, 0.16]	0.14	[−0.14, 0.38]	–	–	–	–
UNADW	0.13	[0.45, −0.19]	1.26	[1.15, 1.39]	0.10	[0.14, 0.06]	−0.07	[−0.23, 0.1]	–	–	–	–
GS	0.02	[0.42, −0.4]	1.90	[1.74, 2.09]	0.01	[0.04, −0.02]	−0.01	[−0.22, 0.21]	–	–	–	–

*Note.* Significant values (bold) are those where the scale factor does not include zero in the 90% confidence interval. Timescales of unfamiliar and unknown are not derived for the non-significant components. Confidence intervals for each scaling and noise are derived via bootstrapping (1,000 resamples), with other confidence intervals derived from these.

The signal, noise, and signal-to-noise ratio for the AMOC and its components are shown numerically in Table 1, with each estimate having 90% confidence intervals estimated by bootstrapping (1,000 resamples). The emergent signals for each component are based on the overall trend of the low-frequency AMOC reflected in each component as defined above for example, approximately, the AMOC shows an overall trend of 1 Sv/decade over the 20 years of RAPID so the signal is 2 Sv. Largest signals are for the AMOC and AMOC—Ek components of 2.04 and 1.78 Sv, respectively. LNADW and thermocline components have the next largest signals at 1.69 and 1.61 Sv, respectively. This can be interpreted that 82% and 78% of the low frequency AMOC signal is reflected in the LNADW and thermocline transports. Lowest signals are in the GS, UNADW, and Ekman components, where signals are not significantly different from zero. Noise levels are highest in the AMOC component, which is not surprising as it is an integrated measure of all components together. The Ekman contribution, has little signal (0.27 Sv) but the noise level is almost 2 Sv. An even lower signal is present in the GS with 0.02 Sv of signal and almost 2 Sv of noise.

When signal and noise are combined, the components with the Ekman transport removed have the highest values. Whilst the signal in the AMOC component has reduced by 0.36 Sv as a result of regressing out Ekman transports, the noise in the AMOC component has decreased by 0.77 Sv equivalent to almost 30%. The AMOC itself is not the component with highest signal-to-noise ratio. Improvements to the signal-to-noise ratio elevate the LNADW — Ek to the top. The noise component for the LNADW dropped by 0.42 Sv or 22% to 1.42 Sv. The LNADW estimate based on deep temperature and salinity measurements shows a lower signal of 1.13 Sv but also lower noise of 1.17 Sv, giving a signal-to-noise ratio of 0.96. Given that this model is simply based on temperature and salinity at a single point on the western boundary of 26°N at 3,000 m depth, this shows 63% of the low frequency AMOC signal is present in the deep western hydrography.

Considering the components that have not had Ekman transport removed, the LNADW and thermocline components have next highest signal-to-noise ratios: 0.87 and 0.84, respectively. Other components have much lower signal-to-noise ratios. All the other components (GS, UNADW, and the Ekman transport) have signal-to-noise ratios of less than 0.15. Overall, the signal-to-noise ratio for all components is low indicating noise swamps

the low frequency AMOC signal for all components. These values are also lower than the “unfamiliar” ( $\text{SNR} > 2$ ) or “unknown” ( $\text{SNR} > 3$ ) thresholds (Frame et al., 2017).

Each of these component transports has a scaling factor ( $\beta$ ) to the low frequency AMOC. Scaling factor estimates of the AMOC itself are by definition close to 1. Deviations from 1 are due to either the removal of Ekman transport or skews in the relationship of the monthly to the low frequency data. Negative scale factors are shown for lower and Upper North Atlantic Deep Water due to the fact that a weakening in AMOC is reflected in these components as less southward transport. There is also a dilution of the signal. The LNADW based on temperature and salinity with Ekman transport removed has a scale factor of  $-0.59$ , showing that trends in this component are half those of the AMOC.

We can use these values to determine when the current trend would become either unfamiliar or unknown. The components with the Ekman transport removed would hit unfamiliar (unknown) around the early 2040s (2060s). Not reducing the noise by removing Ekman transport pushes this threshold back by 5 (10) years, suggesting reduced sensitivity to change.

#### 4. Discussion

We have considered AMOC change using the language of “signal” and “noise” following Hawkins et al. (2020) and Murphy et al. (2023). In this context, we estimate noise as the standard deviations of residuals from a climatic or low frequency signal, using the language of “unfamiliar” and “unknown” for signals that are 2 and 3 standard deviations from a baseline respectively. In comparison with these studies, of the emergence of global temperature trends in local observations, there are a number of very different challenges for the AMOC.

First, the definition of the “signal” is not straight forward. A choice must be made about the level of smoothing applied to data. Again, an analog of the established 30-year window for climate averages is impossible. We have used a 5 years Loess polynomial fitted to the AMOC data as our estimate of low frequency signal. This was found to be the filter length at which most noise estimates began to plateau, with noise estimates not growing more than 0.1 Sv for longer filter lengths. Finally, to calculate a value for the emergent signal, the change based on a linear trend in this signal estimate over the full time period of the estimates was chosen. This is a more conservative choice than the final, low value of the timeseries—a value that could also be subject to boundary bias from fitting.

Second, choosing a baseline or starting point is more ambiguous. Studies of global temperature can employ standard definitions of pre- or early-industrial period of 1850–1900. The same is not possible for AMOC which does not have direct, continuous observations prior to the 21st century. In this study, we have considered a starting point based on the start of RAPID in 2004. Our choice is motivated by the question: if the AMOC does decline due to climate change, when can we start to see this in observations? Moreover, our finding that the noise plateaus after 3 years, indicates that the noise estimate becomes robust and, even if baselines change, the noise—and by extension, the detectability—remains consistent. Thus, we can consider other “signals” and ask when these will emerge.

Results highlight the lack of signal and high noise in the Ekman transport which motivated the removal of Ekman transport from correlated variables. This significantly reduced the noise by 20%–30%, thus improving variables' utility for detecting climatic change. The question could be asked whether more signal may appear in the Ekman component in the future due to changing wind patterns, potentially linked to climate change? This is not supported by climate model analysis and studies have shown that Ekman transports contributes little to future AMOC decline (Asbjørnsen & Årthun, 2023; Beadling et al., 2018; Bryden et al., 2024; Thomas et al., 2012). This is not to say that wind will have no effect on future AMOC, as changes could manifest in wind-driven components such as the GS.

Results also highlight the lack of signal and high noise in the GS. The GS in the RAPID calculation is estimated by the Florida Current timeseries. Recent revisions by Volkov et al. (2024) have led to a reduction of the AMOC signal from previous estimates. So why don't we remove the GS in the same manner as Ekman transport? First, the GS was not seen to covary with the other components as strongly as the Ekman transport. Second, long term studies such as Asbjørnsen and Årthun (2023) and Bryden et al. (2024) have shown that there is a significant contribution of the GS to AMOC decline in climate models. Nonetheless, the lack of signal raises the question of how reconstructions of the GS can be interpreted in an AMOC context (e.g., Piecuch, 2020).

The manifestation of low frequency AMOC change in AMOC components may seem obvious: the components sum to give the AMOC strength and so there must be a relationship. It is therefore surprising perhaps that the Florida Current and UNADW showed little of this low-frequency AMOC signal. LNADW proved a sensitive indicator of low-frequency AMOC change. Using the simple model of Worthington et al. (2021), we were able to recover 60% of the low-frequency AMOC signal in the deep temperature and salinity at the western boundary. This is a powerful result: the full AMOC estimate require multiple moorings across the Atlantic; this deep temperature and salinity are derived from a single location. This shows the importance of deep hydrographic properties in understanding and detecting AMOC change. While a powerful result, it is perhaps not a surprising one: deep density was highlighted as a sensitive indicator of AMOC change by Baehr et al. (2007) in a modeling study shortly after RAPID began.

While deep hydrography is useful for detecting changes in the AMOC, our analysis shows that the signal is reduced by a factor of 0.75 when looking at the full LNADW transports, and by 0.59 when considering LNADW based on deep temperature and salinity (with Ekman transport removed in both cases). This poses a challenge as a climatic AMOC signal may be small. For example, assuming the Atlantic sea surface temperatures are linked to the AMOC, combined with the scaling of 4 Sv/°C relation between AMOC and Atlantic SSTs from Caesar et al. (2018), the signal would be 0.5°C over 2 decades (typical of Atlantic Multidecadal Variability) or a 1 Sv signal in AMOC. This is already close to the limits of hydrographic accuracy as McCarthy et al. (2015) showed that the absolute accuracy of 0.8 Sv (0.6 Sv) for the 10-day (annual) AMOC estimates. Our simple model of LNADW based on temperature and salinity here shows a similar sensitivity. Temperature changes of 0.03°C or salinity changes of 0.004 at 3,000 m on the western boundary are sufficient to change the estimate of LNADW by 1 Sv. This poses a real challenge for salinity calibration as the target accuracy for salinity is 0.003 (temperature calibration has a target accuracy of 0.002°C). This creates difficulties in detecting changes within our current framework and complicates the historical extension of our methodology, especially given the less reliable salinity calibration in the past.

The study questioned whether the 1.0 Sv/decade weakening trend in the RAPID AMOC was significant. In simpler terms, it asked if this weakening led to “unfamiliar” or “unknown” AMOC levels. The answer to both is “no.” We have shown that even in the sensitive estimators of AMOC change—AMOC and LNADW with Ekman noise removed—“unfamiliar” (“unknown”) levels won't be reached by this trend, if it continues, until around the 2040s (2060s). The framework of signal and noise also allows us to consider when larger trends, were they to occur, would emerge from the noise. For example, a 5 Sv/year weakening trajectory is consistent with the mid-21st century collapse of the AMOC discussed by Ditlevsen and Ditlevsen (2023). Were this to occur, unfamiliar (unknown) values of AMOC would emerge in around 10 (15) years, given an estimated noise level of 2.5 Sv in AMOC values when seasonality and Ekman influence is removed. In other words, if this extreme scenario were to occur, RAPID would detect it by the end of the decade. Looking at AMOC estimates from 2018, a 5 Sv/yr trend has been seen in the RAPID data (Figure 2a), were this trend to continue, in another 2–3 years, AMOC values would reach the unfamiliar level.

## 5. Conclusions

We have considered observed AMOC change at the RAPID array in a signal to noise framework and conclude that we have yet to see AMOC values that are “unfamiliar” or much less “unknown.” We have explored the sensitivity of observations in the RAPID array to detection of signals and emphasize the importance of removing those components that carry much noise and little signal such as Ekman transport. In our framework, the overall trend from RAPID of 1.0 [0.6–1.4] Sv/decade, which is close to the estimate of future AMOC weakening from climate models (Weijer et al., 2020), will result in unfamiliar values by around 2040 and unknown values by 2060.

Our confidence in these future climate projections is typically based on a climate model's ability to reproduce the past—something that climate models are not so good at for AMOC (McCarthy and Caesar 2023)—and that past AMOC strength is a controversial topic in its own right (Caesar et al., 2021; Kilbourne et al., 2022). Whether or not the AMOC has been declining overall since the mid-20th century depends heavily on whether or not the AMOC was stronger in the first half of the 20th century (Caesar et al., 2021). In this study, we have highlighted the potential for deep hydrography, near the western boundary of the Atlantic to provide a sensitive estimate of low-frequency AMOC variations and offers the potential to reconstruct the AMOC in the past, although challenges around calibration remain.



Nonetheless, the challenge in detecting climatic change in the AMOC is significant. The noise is large and the signal may be small. This emphasizes the importance of high quality direct observations of the AMOC such as those provided by RAPID since 2004, not only as a tool for monitoring the AMOC in the present but also for understanding the past and independently contextualizing future projections.

### Conflict of Interest

The authors declare no conflicts of interest relevant to this study.

### Data Availability Statement

All data used in this study are freely available on <https://rapid.ac.uk/data/data-download/>. Two data files are necessary for the calculations in this paper: MOC transports in ASCII format and Gridded TS profiles in NetCDF format. Code used in the calculations here and for the generation of figures was developed in the freely available R language and is available at [https://github.com/gerardmccarthy/rapid\\_snr\\_code](https://github.com/gerardmccarthy/rapid_snr_code).

### Acknowledgments

We would like to thank Chris Piecuch and an anonymous reviewer for their comments that greatly improved this manuscript. We would like to express great appreciation to all who have been involved in maintaining the RAPID-MOCHA-WBTS array, including collecting data at sea. GM and KM are supported by the A4 Project (Aigéin, Aeráid, agus athrú Atlantaigh), with the support of the Marine Institute, under the Marine Research Programme, funded by the Irish Government Grant PBA/CC/18/01). GM and GH are supported by iCRAG, with the support of Science Foundation Ireland (Grant 13/RC/2092\_P2). BM and DS are supported by Natural Environment Research Council Grants NE/Y003551/1 and NE/Y005589/1.

### References

- Asbjørnsen, H., & Årthun, M. (2023). Deconstructing future AMOC decline at 26.5°N. *Geophysical Research Letters*, 50(14), e2023GL103515. <https://doi.org/10.1029/2023GL103515>
- Baehr, J., Haak, H., Alderson, S., Cunningham, S. A., Jungclauss, J. H., & Marotzke, J. (2007). Timely detection of changes in the meridional overturning circulation at 26°N in the Atlantic. *Journal of Climate*, 20(23), 5827–5841. <https://doi.org/10.1175/2007JCLI1686.1>
- Beadling, R. L., Russell, J. L., Stouffer, R. J., & Goodman, P. J. (2018). Evaluation of subtropical North Atlantic ocean circulation in CMIP5 models against the observational array at 26.5°N and its changes under continued warming. *Journal of Climate*, 31(23), 9697–9718. <https://doi.org/10.1175/JCLI-D-17-0845.1>
- Bellomo, K., Angeloni, M., Corti, S., & von Hardenberg, J. (2021). Future climate change shaped by inter-model differences in Atlantic meridional overturning circulation response. *Nature Communications*, 12(1), 3659. <https://doi.org/10.1038/s41467-021-24015-w>
- Bryden, H., Beunk, J., Drijfhout, S., Hazeleger, W., & Mecking, J. (2024). Comparing observed and modelled components of the Atlantic meridional overturning circulation at 26°N. *Ocean Science*, 20(2), 589–599. <https://doi.org/10.5194/OS-20-589-2024>
- Caesar, L., McCarthy, G. D., Thornalley, D. J. R. R., Cahill, N., & Rahmstorf, S. (2021). Current Atlantic meridional overturning circulation weakest in last millennium. *Nature Geoscience*, 14(3), 118–120. <https://doi.org/10.1038/s41561-021-00699-z>
- Caesar, L., Rahmstorf, S., Robinson, A., Feulner, G., & Saba, V. (2018). Observed fingerprint of a weakening Atlantic Ocean overturning circulation. *Nature*, 556(7700), 191–196. <https://doi.org/10.1038/s41586-018-0006-5>
- Chidichimo, M. P., Kanzow, T., Cunningham, S. A., Johns, W. E., & Marotzke, J. (2010). The contribution of eastern-boundary density variations to the Atlantic meridional overturning circulation at 26.5°N. *Ocean Science*, 6(2), 475–490. <https://doi.org/10.5194/os-6-475-2010>
- Cunningham, S. A., Kanzow, T., Rayner, D., Baringer, M. O., Johns, W. E., Marotzke, J., et al. (2007). Temporal variability of the Atlantic meridional overturning circulation at 26.5°N. *Science (80-. )*, 317(5840), 935–938. <https://doi.org/10.1126/science.1141304>
- Ditlevsen, P. D., & Ditlevsen, S. (2023). Warning of a forthcoming collapse of the Atlantic meridional overturning circulation. *Nature Communications*, 14(14), 1–12. <https://doi.org/10.1038/s41467-023-39810-w>
- Evans, D. G., Frajka-Williams, E., & Naveira Garabato, A. C. (2022). Dissipation of mesoscale eddies at a western boundary via a direct energy cascade. *Scientific Reports* 2022, 12(12), 1–13. <https://doi.org/10.1038/s41598-022-05002-7>
- Frajka-Williams, E., Anson, I. J., Baehr, J., Bryden, H. L., Chidichimo, M. P., Cunningham, S. A., et al. (2019). Atlantic meridional overturning circulation: Observed transport and variability. *Frontiers in Marine Science*, 6, 260. <https://doi.org/10.3389/fmars.2019.00260>
- Frajka-Williams, E., Meinen, C. S., Johns, W. E., Smeed, D. A., Duchez, A., Lawrence, A. J., et al. (2016). Compensation between meridional flow components of the Atlantic MOC at 26°N. *Ocean Science*, 12(2), 481–493. <https://doi.org/10.5194/OS-12-481-2016>
- Frame, D., Joshi, M., Hawkins, E., Harrington, L. J., & De Roiste, M. (2017). Population-based emergence of unfamiliar climates. *Nature Climate Change*, 22(6), 407–411. <https://doi.org/10.1038/NCLIMATE3297>
- Hawkins, E., Frame, D., Harrington, L., Joshi, M., King, A., Rojas, M., & Sutton, R. (2020). Observed emergence of the climate change signal: From the familiar to the unknown. *Geophysical Research Letters*, 47(6), e2019GL086259. <https://doi.org/10.1029/2019GL086259>
- IPCC. (2019). Special report on the ocean and Cryosphere.
- IPCC. (2021). *Climate change 2021: The physical science basis. Working Group I Contribution to the IPCC Sixth Assessment Report*.
- Jackson, L. C., Kahana, R., Graham, T., Ringer, M. A., Woollings, T., Mecking, J. V., & Wood, R. A. (2015). Global and European climate impacts of a slowdown of the AMOC in a high resolution GCM. *Climate Dynamics*, 45(11–12), 3299–3316. <https://doi.org/10.1007/s00382-015-2540-2>
- Kanzow, T., Cunningham, S. A., Johns, W. E., Hirschi, J. J. M., Marotzke, J., Baringer, M. O., et al. (2010). Seasonal variability of the Atlantic meridional overturning circulation at 26.5°N. *Journal of Climate*, 23(21), 5678–5698. <https://doi.org/10.1175/2010JCLI3389.1>
- Kanzow, T., Johnson, H. L., Marshall, D. P., Cunningham, S. A., Hirschi, J.-M., Mujahid, A., et al. (2009). Basinwide integrated volume transports in an eddy-filled ocean. *Journal of Physical Oceanography*, 39(12), 3091–3110. <https://doi.org/10.1175/2009jpo4185.1>
- Kilbourne, K. H., Wanamaker, A. D., Moffa-Sanchez, P., Reynolds, D. J., Amrhein, D. E., Butler, P. G., et al. (2022). Atlantic circulation change still uncertain. *Nature Geoscience*, 15(3), 165–167. <https://doi.org/10.1038/s41561-022-00896-4>
- Lobelle, D., Beaulieu, C., Livina, V., Sévellec, F., & Frajka-Williams, E. (2020). Detectability of an AMOC decline in current and projected climate changes. *Geophysical Research Letters*, 47(20), e2020GL089974. <https://doi.org/10.1029/2020GL089974>
- McCarthy, G., Frajka-Williams, E., Johns, W. E., Baringer, M. O., Meinen, C. S., Bryden, H. L., et al. (2012). Observed interannual variability of the Atlantic meridional overturning circulation at 26.5°N. *Geophysical Research Letters*, 39(19), L19609. <https://doi.org/10.1029/2012gl052933>
- McCarthy, G. D., & Caesar, L. (2023). Can we trust projections of AMOC weakening based on climate models that can't reproduce the past? *Philosophical Transactions of the Royal Society A*, 381(2262), 20220193. <https://doi.org/10.1098/rsta.2022.0193>

- McCarthy, G. D., Smeed, D. A., Johns, W. E., Frajka-Williams, E., Moat, B. I., Rayner, D., et al. (2015). Measuring the Atlantic meridional overturning circulation at 26°N. *Progress in Oceanography*, *31*, 91–111. <https://doi.org/10.1016/j.pocean.2014.10.006>
- Moat, B. I., Smeed, D. A., Frajka-Williams, E., Desbruyères, D. G., Beaulieu, C., Johns, W. E., et al. (2020). Pending recovery in the strength of the meridional overturning circulation at 26°N. *Ocean Science*, *16*(4), 863–874. <https://doi.org/10.5194/OS-16-863-2020>
- Moat, B. I., Smeed, D. A., Rayner, D., Johns, W. E., Smith, R., Volkov, D., et al. (2024). *Atlantic meridional overturning circulation observed by the RAPID-MOCHA-WBTS (RAPID-Meridional overturning circulation and Heatflux array-western boundary time Series) array at 26N from 2004 to 2023 (v2023.1)*. British Oceanographic Data Centre - Natural Environment Research Council, UK. <https://doi.org/10.5285/223b34a3-2dc5-e945-e063-7086abc0f274>
- Murphy, C., Coen, A., Clancy, I., Decristoforo, V., Cathal, S., Healion, K., et al. (2023). The emergence of a climate change signal in long-term Irish meteorological observations. *Weather and Climate Extremes*, *42*, 100608. <https://doi.org/10.1016/J.WACE.2023.100608>
- Pérez-Hernández, M. D., McCarthy, G. D., Vélez-Belchí, P., Smeed, D. A., Fraile-Nuez, E., & Hernández-Guerra, A. (2015). The canary basin contribution to the seasonal cycle of the Atlantic meridional overturning circulation at 26°N. *Journal of Geophysical Research: Ocean*, *120*(11), 7237–7252. <https://doi.org/10.1002/2015JC010969>
- Piecuch, C. G. (2020). Likely weakening of the Florida Current during the past century revealed by sea-level observations. *Nature Communications*, *11*(1), 3973. <https://doi.org/10.1038/s41467-020-17761-w>
- Roberts, C. D., Jackson, L., & McNeill, D. (2014). Is the 2004–2012 reduction of the Atlantic meridional overturning circulation significant? *Geophysical Research Letters*, *41*(9), 3204–3210. <https://doi.org/10.1002/2014gl059473>
- Roberts, C. D., Waters, J., Peterson, K. A., Palmer, M., McCarthy, G. D., Frajka-Williams, E., & Haines, K. (2013). Atmosphere drives recent interannual variability of the Atlantic meridional overturning circulation at 26.5°N. *Geophysical Research Letters*, *40*, 10. <https://doi.org/10.1002/grl.50930>
- Smeed, D. A., McCarthy, G. D., Cunningham, S. A., Frajka-Williams, E., Rayner, D., Johns, W. E., et al. (2014). Observed decline of the Atlantic meridional overturning circulation 2004 to 2012. *Ocean Science*, *10*, 38–39. <https://doi.org/10.5194/os-10-29-2014>
- Thomas, M. D., De Boer, A. M., Stevens, D. P., & Johnson, H. L. (2012). Upper ocean manifestations of a reducing meridional overturning circulation. *Geophysical Research Letters*, *39*(16), L16609. <https://doi.org/10.1029/2012GL052702>
- Volkov, D. L., Smith, R. H., Garcia, R. F., Smeed, D. A., Moat, B. I., Johns, W. E., & Baringer, M. O. (2024). Florida Current transport observations reveal four decades of steady state. *Nature Communications*, *15*(1), 1–12. <https://doi.org/10.1038/s41467-024-51879-5>
- Weijer, W., Cheng, W., Garuba, O. A., Hu, A., & Nadiga, B. T. (2020). CMIP6 models predict significant 21st century decline of the Atlantic meridional overturning circulation. *Geophysical Research Letters*, *47*(12), e2019GL086075. <https://doi.org/10.1029/2019GL086075>
- Worthington, E. L., Moat, B. I., Smeed, D. A., Mecking, J. V., Marsh, R., & McCarthy, G. D. (2021). A 30-year reconstruction of the Atlantic meridional overturning circulation shows no decline. *Ocean Science*, *17*(1), 285–299. <https://doi.org/10.5194/os-17-285-2021>